JOURNAL OF THE ATMOSPHERIC SCIENCES

Non-uniqueness in a Single Column Model for Moist Convection

M.R. TURNER[1]* AND J. NORBURY[2]

[1] *Department of Mathematics, University of Surrey, Guildford, Surrey GU2 7XH, UK*
[2] *Mathematical Institute, University of Oxford, Andrew Wiles Building, Woodstock Road, Oxford OX2 6GG, UK*

ABSTRACT

We investigate a moist atmospheric column convection model by considering the atmosphere as a single vertical column of air parcels, each of which contains water vapour. The moist convective adjustment of both air and water mass in the column is considered from an (unstable) initial state to a statically stable final configuration of parcels. Two variations of an algorithm based upon swapping neighbouring parcels are compared: after swapping, no parcels remain supersaturated. The results of these algorithms are compared directly with those of the adjustment algorithm of Cheng *et al.* 2017 (*Q. J. R. Meteorol. Soc.* **143**(708) p. 2925-2939) which adjusts an atmospheric column to achieve the global maximum of a relevant cost functional. Two examples are considered: in the first,the algorithms adjust to similar arrangements, showing that the global maximum of the functional is the dynamically preferred state, while in the second, the algorithms adjust to significantly different states. Thus we identify a non-uniqueness to the solution to the adjustment problem in terms of local and global cost functional maximisers. We then discuss the relevance of this non-uniqueness to numerical prediction in weather and climate models.

1. Introduction

The accurate numerical prediction of weather and climate events requires the solution of the full, compressible Navier-Stokes equations within a narrow layer of atmosphere surrounding the Earth, coupled with differential equations which govern physical processes such as the movement of heat energy and condensational phase changes of water vapour in the air. The number of degrees of freedom involved in this numerical prediction problem is immense, and it is unlikely that even the next generation of computer architecture will be able to simulate all the time and length scales of cumulus cloud behaviour in this system accurately. To overcome this problem, temporally and spatially averaged forms of the governing equations are solved numerically on fixed spatial grids of more than one kilometre in the horizontal direction. While this makes the numerical solution to the system tractable, it means that weather and climate events occurring on scales below the resolution scales of the averaged system need to be added back into the system in an 'averaged' sense via parameterizations of the sub-grid scale behaviour.

An important sub-grid scale phenomenon which needs parameterizing in this way is moist cumulus convection (Arakawa 2004). This phenomenon plays a significant role in the vertical fluxes of entropy, air mass, moisture and air momentum in the atmosphere, each of which can have large magnitudes. This is particularly the case in the tropical regions of the Earth's atmosphere where these fluxes make an important contribution to the tropical circulation. This tropical circulation in turn helps to drive the Earth's climate. Currently it is only possible to directly represent convection in weather and climate simulations with grid blocks which are (at least) 1-2 km in horizontal length, and often much more than this. Today's general circulation models (GCMs) are typically running with a horizontal spatial grid resolution of 10 km at most. Hence we are a long way from the direct representation of convection in these models (the horizontal column footprints of approximately 100 square kms need to be reduced to the order of 1 square km). One useful approach to modeling the small scale effects of moist convection, and understanding its effect on the larger scale dynamics of the system, is to consider one-dimensional single-column-atmosphere models developed (and investigated) by Yanai et al. (1973), see also Tiedtke (1989) and references therein.

Single-column-atmosphere models are simplified atmosphere models where physical processes such as moist convection or vertical heat transfer can be explored without directly simulating the large scale horizontal dynamics (see Sobel and Bretherton (2000); Ghan et al. (2000) and references therein for more details). These single-column models have formed a significant part of many theoreti-

*Corresponding author address: Department of Mathematics, University of Surrey, Guildford, Surrey GU2 7XH, UK
E-mail: m.turner@surrey.ac.uk

cal convection studies due to their ability to sensibly and accurately model convective processes while retaining a simple one-dimensional structure (Shutts 1994; Holt 1989; Lock and Norbury 2011; Cheng et al. 2017a,b). Such single column models are readily used in GCMs, but due to 'functional' errors in these models, which take the form of model biases and unwanted trade-offs (Bretherton 2007), their modelling of reality is still under some scrutiny. For example, they can lead to a weak or missing Madden-Julian oscillation (Madden and Julian 1971), and in particular, they are poor at predicting the diurnal transition between shallow and deep convection (Yang and Slingo 2001; Betts and Jakob 2002). Here we define shallow convection as non- or weakly-precipitating convection which is usually restricted to the lower half of the troposphere, while deep convection is heavily-precipitating convection that typically approaches the tropopause. Many single column convection schemes parametrize deep and shallow convection separately, but this is undesirable because in the physical atmosphere the transition from shallow to deep convection is a seamless process in both space and time. Hence it is desirable to have a unified scheme which incorporates both convection processes. There has been some progress in this direction over the last decade but this problem is by no means solved (Hohenegger and Bretherton 2011; Mapes and Neale 2011; Park 2014; D'Andrea et al. 2014). Here we examine a unified single column model wherein deep and shallow convection events occur as different possible solutions to the same initial problem.

The particular parametrization scenario we consider is similar to that in Cheng et al. (2017a) which is a single column of compressible air parcels (an air parcel is a mass of air with homogeneous properties of gas density, heat energy and moisture density). Cheng et al. (2017a) devised a numerical algorithm which instantaneously adjusts the parcels from an initial buoyantly unstable configuration into a final statically stable (nowhere supersaturated) state. Such an unstable configuration can be triggered, for example, either (i) by a buoyantly stable column being lifted when passing over mountain topography, causing initially moist but unsaturated parcels to become supersaturated, and hence unstable; or (ii) by an unsaturated column becoming buoyantly unstable due to surface heating. The adjustment removes any instability from the column by moving parcels to a statically (buoyantly) stable arrangement which is nowhere supersaturated. Note, at no point does this approach solve the underlying three-dimensional (possibly turbulent) vertical dynamics, it solely models the physical laws of convection (i.e. the conserved thermodynamic processes) on unresolved short-time-scales via the transportation of air parcels.

In GCMs for weather and climate simulations, the vertical thermodynamic structure of the atmosphere generally needs to be 'adjusted' at each time step so that the atmosphere is stable (or sufficiently stable) in the vertical direction so that the next time step can be applied. In current simulations the adjustment phase typically uses an algorithm based upon the Moist Available Potential Energy (MAPE) (or Available Potential Energy (APE)), with the columnar atmosphere considered as a single columnar plume (Randall and Wang 1992; Wang and Randall 1994). The MAPE of a single column (or, sometimes, a slightly more complex domain) gives an upper bound on the amount of kinetic energy produced through latent heating only, and is found by determining the global minimum total potential energy configuration of the air parcels. However, the single atmospheric plume construction is not always representative of the actual atmosphere, and in fact satellite observations show clouds forming in multiple layers, implying that the underlying process can be more complicated than a single plume. Various non-plume numerical weather and climate prediction schemes use an adjustment process based upon the Convective Available Potential Energy (CAPE). This approach calculates the available energy of a single (small) air parcel as it rises in the column (Emanuel 1994; Riemann-Campe et al. 2009). However, MAPE is usually preferred to CAPE because MAPE accounts for both ascending and descending air (Lorenz 1979; Randall and Wang 1992; Wang and Randall 1994). The algorithm presented by Cheng et al. (2017a) also deals with both upward and downward moving air parcels, and is based upon physical conservation laws, specifically those of air mass, thermal energy and moisture mass. For the convection process, in a column which does not lose or gain energy via radiation, Cheng et al. (2017a) conserve the quantities θ for unsaturated parcels and $\theta^M := \theta + Lq$ for saturated parcels. Here θ is the potential temperature, q is the specific humidity (of the water vapour in the parcel) and L is a physical constant which is large to denote that condensation of small amounts of water vapour leads to large increases in the potential temperature. These conserved quantities are suitable approximations (such as linearizations) of the exact conserved thermodynamic quantities when q is small, but in this paper we use more accurate forms of these thermodynamic conserved quantities in order to construct a more quantitatively accurate adjustment algorithm. The Cheng et al. (2017a) adjustment algorithm simultaneously rearranges all the parcels, with no defined order of parcel sorting; it assumes parcels remain saturated even when they may have been overtaken by other faster moving parcels, and it neglects any effect of the parcels moving during the adjustment phase. As saturated parcels move upwards they conserve θ^M by condensing water vapour (decreases q) while simultaneously releasing latent heat (increases θ); L is the conversion factor for this process.

The algorithm of Cheng et al. (2017a) transforms some pre-adjusted state, comprising saturated, supersaturated and buoyantly unstable parcels, to a stable adjusted state,

where no parcel is supersaturated. For certain initial data scenarios, the final stable state is a *weak* adjustment solution where the column is made up of vertical stacks of pancake-like regions interleaving moist and dry parcels, similar to appropriate relevant states observed in the real atmosphere, such as in lenticular clouds which form in laminar layers on the downside of mountains (Houze 1993; Whiteman 2000; Neiman and Shaw 2003). Formulations of the convection problem in columns of the atmosphere have the property that these new fine scaled, vertically layered solutions may exist; these so-called *weak* solutions cannot be found using differential equation models, which average over these fine layers to get more continuously varying solutions. The usual numerical methods require a certain smoothness of solutions so that higher derivatives exist. Here the new solutions interleave dry and moist parcels such that the moisture field is not even continuous, let alone differentiable. In modern PDE jargon these are known as weak solutions; somewhat surprisingly these mathematically curious solutions can be seen in actual atmospheric scenarios, so it is a success of these column adjustment algorithms that they can computationally approximate these new solutions that may be of practical forecasting value. The results in Cheng et al. (2017a), including those with the interleaving weak solution, were shown to arise from the global maximum of an integral cost functional, which was confirmed by directly numerically maximising the particular functional using the Munkres algorithm. The adjustment algorithm of Cheng et al. (2017a) is related to the simpler incompressible, Boussinesq, individual-parcel-sorting algorithm of Cheng et al. (2017b), which provides a proof of the well-posed convergence to weak solutions of the original PDE problem in the limit as the time-step of the time-dependent problem $\Delta t \to 0$. In the limit $\Delta t \to 0$ the algorithms of Cheng et al. (2017a) and Cheng et al. (2017b) coincide.

The algorithm presented in Cheng et al. (2017a) behaves similarly to those algorithms assessed in Stansifer et al. (2017) and Harris and Tailleux (2018) in that it computes a parcel arrangement which globally maximizes (or minimizes) some integral functional. Here we propose a different adjustment algorithm (to that of Cheng et al. (2017a)) which seeks to find local maxima of the same cost functional. Rather than sorting all parcels simultaneously, we propose an algorithm which sorts parcels by swapping neighbouring parcels one by one in a clearly defined order. Such an algorithm allows us to consider other such local adjustments of the column, different to the global adjustment of Cheng et al. (2017a), from a given pre-adjusted state. In particular we demonstrate that the parcel swapping algorithm delivers a potentially more appropriate (in terms of practical weather and climate forecasting) adjustment of the column for certain pre-adjusted states, and delivers the same adjustment for other initial states. It also allows for scenarios where an ascending parcels overtakes a saturated parcel, forcing it down the column and hence making it unsaturated. This effect is not present in Cheng et al. (2017a). This then poses the question, if more than one adjustment from the same initial data to different final adjusted states can be found via different algorithms (a shallow convection verses deep convection event perhaps), which one is more appropriate for a given time-step in a numerical weather prediction simulation? As well as computing multiple adjusted solutions for the same pre-adjusted state, a feature of the proposed parcel-swapping algorithm is that it provides a sounder physical basis for implementing the convective inhibition criterion (CIC) (Colby Jr 1984). This criterion states that an ascending parcel requires sufficient buoyancy in order to swap with its neighbouring parcel directly above. In the Cheng et al. (2017a) algorithm this criterion was implemented only in an approximate way, because sorting all parcels simultaneously makes it difficult to identify the levels in the column where each ascending parcel moves above other stationary or descending parcels.

This paper is laid out as follows. In §2 the moist convection problem is presented along with the formulation of the problem in terms of physical conservation laws for mass (of both air and moisture) and thermal energy as measured by the moist potential temperature. In §3 we describe the new parcel swapping algorithm used to find the adjusted, stable equilibrium state (or states) of an initially unstable atmosphere. Results of this algorithm showing the non-unique nature of the adjustment problem are presented in §4, with a discussion on the implications of these results in §5.

2. Formulation

Consider a single (vertical in height z) atmospheric column of moist air situated at a particular longitude and latitude on the Earth's surface and bounded between pressures $p \in [p_0, p_{\text{top}}]$. The column is assumed to satisfy the ideal gas in hydrostatic balance, thus $\frac{\partial p}{\partial z} = -\rho(T,p)g$ where the density $\rho(T,p)$ satisfies the approximate ideal gas law for the pressure $p = \rho R(1+0.608q)T$ (see p41 Gill (1982)). Here T is the absolute temperature, $R = 287\,\text{J}\text{kg}^{-1}\text{K}^{-1}$ is the dry air gas constant, $g = 9.81\,\text{ms}^{-2}$ is the gravitational constant and $q = \rho_v/\rho$ denotes the specific humidity for moist air with vapour density ρ_v. For convenience we introduce the virtual temperature $T_v = (1+0.608q)T$ which is the temperature at which dry air ($q = 0$) would have the same density as moist air at a given pressure, assuming ideal gas behaviour.

Rather than using z as the vertical coordinate, it is more convenient to use pressure, as then equal sized pressure parcels of air contain the same mass of air, thus swapping parcels in our numerical scheme (automatically) conserves mass of air in the column. In the column itself, the p-axis (or z-axis) is orientated vertically, that is, perpendicular

to the Earth's geoid surface, and the column contains two locally horizontally connected regions. One region (the *pseudo-adiabat*) contains the upward motion in the column, and the other (the *environment*) contains the downward motion. The pseudo-adiabat tends to have a much smaller relative volume within the column compared to the environment because the upward motion tends to be much faster than the downward motion, but typically the ratio of these volumes is unknown. Hence rather than model each region separately, we simultaneously model the respective upward and downward motions (Lock and Norbury 2011), and this provides the mechanism that allows parcels to pass through each other.

Following Gill (1982), Emanuel (1994) or Pierrehumbert (2010), the first law of thermodynamics for an unsaturated atmosphere shows that for an ascending parcel of air mass, the virtual potential temperature

$$\theta_v = T_v \left(\frac{p_0}{p}\right)^{R/c_p}, \tag{1}$$

is conserved for adiabatic processes. Here $c_p = 1004\ \mathrm{J kg^{-1} K^{-1}}$ is the dry air specific heat constant at a given constant pressure. Note, equivalently we can define the dry $(q = 0)$ potential temperature as $\theta = T\left(\frac{p_0}{p}\right)^{R/c_p}$, so that $\theta_v \to \theta$ as $q \to 0$. For ascending air parcels in a saturated moist atmosphere, the equivalent potential temperature

$$\theta_e = \theta \exp\left(\frac{Lq}{T}\right), \tag{2}$$

is conserved even if water vapour condenses during the motion (see p51 of Gill (1982), p120 Emanuel (1994) or the chapter on thermodynamics (for planetary atmospheres) made easy in Pierrehumbert (2010)).

Other physical processes such as the net radiative heating/cooling of air parcels can be incorporated into the governing thermodynamic equations for practical applications, and in this case the governing quantities θ_v and θ_e will no longer be simply conserved. Instead the evolution of these quantities will be governed by differential equations (see Lock and Norbury (2011) for a theoretical example for a Boussinesq atmosphere). In this article our primary focus is solely on the latent heat release and we assume that the movement of parcels occurs on a 'seconds' timescale much faster than effects such as daily column heating/cooling, which can hence be neglected for simplicity. The physical constant appearing in (2) $L = L_v/c_p = 2490\,\mathrm{K}$, is the conversion factor which determines the increase in potential temperature within an air parcel when some fraction of the water vapour it contains is converted into liquid water at the same temperature. Here the constant L_v is the latent heat of vaporization (condensation). In practical applications cloud generation with various forms of precipitation are also modelled, but here it is assumed that vapour goes directly to rain (which is then removed from the system) for simplicity. This removal of rain means that not only are the types and forms of melted/frozen precipitation not relevant, but that crucially we do not consider re-evaporation to drier parcels here.

We consider an atmospheric column with no fluxes (of either gas mass, moisture or thermal energy) at the top or bottom. We define a *statically stable* column as one with

$$\frac{\partial \theta_v}{\partial p} \leq 0, \tag{3}$$

through the entire column, which is equivalent to $\frac{\partial \theta_v}{\partial z} \geq 0$. The reason for including the stability condition (often referred to as dry stability even when moisture is present, provided the parcels are unsaturated) in terms of both independent coordinates is because here we find it more intuitive to plot the results as a function of the height variable z. The pressure and height variables are connected here via the ideal gas law in hydrostatic balance

$$\frac{\partial p}{\partial z} = -\frac{g p_0}{R\theta_v(p)} \left(\frac{p_0}{p}\right)^{R/c_p - 1},$$

which can be integrated to give the height variable

$$z(p) = -\frac{R}{g p_0} \int_{p_0}^{p} \theta_v(p') \left(\frac{p_0}{p'}\right)^{1 - R/c_p} \mathrm{d}p'. \tag{4}$$

The origin of the (strong) nonlinearity of the problem comes from the fact that supersaturated/saturated ($q \geq Q_{\mathrm{sat}}$) air parcels have the potential to convert moisture into latent heat causing them to ascend the column releasing CAPE, while unsaturated air parcels do not. Therefore, while condition (3) is sufficient for the dry (non-saturated) stability of the column, if any parcels are saturated or supersaturated there could potentially be alternative stable rearrangements of the air parcels in the column, determined by allowing parcels to condense moisture, take on the released heat energy, and rise. These alternative arrangements of parcels must also satisfy (3), with $q \leq Q_{\mathrm{sat}}$ everywhere, in order for them to be stable. Here the function $Q_{\mathrm{sat}}(T, p)$ denotes the saturation specific humidity for condensation given by the Clausius-Clapeyron relation (Gill 1982), defined explicitly later in (12). Water vapour with $q > Q_{\mathrm{sat}}$ is assumed to quickly condense out as rain so that $q = Q_{\mathrm{sat}}$; effectively q lowers to Q_{sat}, and then $q = Q_{\mathrm{sat}}$ holds during any rising of the parcel with appropriate condensation so that θ_e is constant.

In the physical atmosphere, complicated three-dimensional adjustment processes determine the transport of temperature and specific humidity, and to model this would require the time-integration of the fully three-dimensional Navier-Stokes equations. In this work we replace this complex process by the vertical transport of individual air parcels, where the horizontal dynamics in the

column is left un-modelled. Modelling this complicated 3D motion as an instantaneous parcel response means that we can allow parcels to move a finite distance in apparently zero time. While this appears unphysical, what it really means is the adjustment process is considered to occur on a faster timescale to the background dynamics (minutes to hours), which is consistent with the physical atmosphere in most practical (seconds to minutes) adjustment scenarios. This type of adjustment model has some similarities to mass-flux convection schemes such as in Tiedtke (1989) and Gregory and Rowntree (1990), however, in our adjustment model we do not model or solve for the ascending parcel dynamics, parcels are assumed to swap or jump to their new level instantaneously. Our model also neglects any mixing of the air parcels, or feedback from the condensing moisture, it makes no assumptions on entrainment rates between the environment and pseudo-adiabat, and condensed moisture is assumed to rain out of the system immediately. The model only uses actual values of θ_v, θ_e and q, capturing the leading order effect of moisture condensation in the atmosphere and its effect on the atmosphere column stability.

We consider the air column to be discretized into a vertical one-dimensional array of air parcels, and we consider the movement of the parcels in a Lagrangian-parcel-following sense (Emanuel 1994; Bokhove and Oliver 2006; Cheng et al. 2017a) via the conservation of the quantities θ_v and θ_e in (1) and (2). Thus we have the two scenarios:

- For unsaturated parcels ($q < Q_{\rm sat}$)

$$\begin{aligned} &q_A = q(p_A(t),t) = q(p_A(0),0), \text{ and} \\ &\theta_{vA} = \theta_v(p_A(t),t) = \theta_v(p_A(0),0), \quad \forall A, \end{aligned} \tag{5}$$

  at time t, where $p = p_A(t)$ is the pressure location of the parcel with Lagrangian label A. The unsaturated parcels move adiabatically and tend to be forced down in a column as saturated parcels release moisture, gain latent heat, and rise above them. However the parcels can adjust and ascend the column if (3) does not hold everywhere - if during their ascent they become saturated they then follow the process in the bullet point below.

- For saturated parcels ($q = Q_{\rm sat}$), conservation of (2) means

$$\begin{aligned} &\theta_A \exp\left(\frac{Lq_A}{T_A}\right) = \\ &\theta_A(p_A(0),0)\exp\left(\frac{Lq_A(p_A(0),0)}{T_A(p_A(0),0)}\right) = \theta_{eA} \ \ \forall A, \end{aligned} \tag{6}$$

  as the parcel ascends along the curve $T\left(\frac{p_0}{p}\right)^{R/c_p}\exp\left(\frac{LQ_{\rm sat}(T,p)}{T}\right) = \theta_{eA}$ in the (T,p)-plane (denoted by $C(A)$- this is the moist adiabat) for each parcel A. Therefore condensed moisture is accompanied by a latent heat increase (with the conversion factor L) for the parcel as it ascends.

Any saturated parcel with Lagrangian label A will remain on $C(A)$ as it ascends in the column, which means that while it condenses water vapour it also remains saturated. The curve $C(A)$ is often termed the moist adiabat and along this curve a parcel, originally at pressure p_A, with equivalent potential temperature θ_{eA}, which rises to a level p_B then has absolute temperature, T_B, given by the solution to the implicit equation

$$T_B\left(\frac{p_0}{p_B}\right)^{R/c_p}\exp\left(\frac{LQ_{\rm sat}(T_B,p_B)}{T_B}\right) = \theta_{eA}. \tag{7}$$

The form of $Q_{\rm sat}(T,p)$ applicable for the Earth's atmosphere that we use is given in (12): it is based on an approximation from Gill (1982) that is used in our (semi-analytic) solution to make the procedure simpler to understand.

3. Numerical moist convection adjustment algorithm

If the atmospheric column is buoyantly unstable, i.e. if (3) is violated anywhere in the column, or if the atmosphere is buoyantly stable, but contains parcels which are supersaturated, then the air parcels within the column adjust their positions (via the unresolved dynamics) to remove the instability. During this process the column is said to be *convectively adjusted* into a new stable state. For a column of unsaturated parcels ($0 \le q < Q_{\rm sat}(T,p)$ for all times), the final stable parcel arrangement within the column is unique, with θ_v ordered monotonically as we ascend the column,with the hottest parcels at the top of the column (Shutts and Cullen 1987). However, for a column with saturated/supersaturated parcels there are potentially more than one stable re-arrangement which satisfies (3) and has $q \le Q_{\rm sat}$ everywhere.

Cheng et al. (2017a) developed a moist convective adjustment algorithm which sorted an initial configuration of parcels into a new configuration simultaneously, starting from the top of the column and working down to the bottom. Note, in their algorithm the conserved quantities considered were the potential temperature, θ, for unsaturated parcels and the combination $\theta + Lq$ for saturated parcels, also their stability condition (3) was given in terms of θ. Essentially these quantities are the small q approximations of (1) and (2) close to the surface of the Earth, and were used to highlight the potential solution structures which can develop in this system. The same algorithm used in Cheng et al. (2017a) can be used to conserve the quantities (1) and (2) with minimal modification and we expect qualitatively similar results to Cheng et al. (2017a) here. The algorithm in Cheng et al. (2017a) allowed each parcel to ascend to the working height and, as long as a

simplification of the convective inhibition criterion (CIC) was satisfied, the parcel with the largest potential temperature at the working height, after taking into account latent heating, was installed at that height. The results of the Cheng et al. (2017a) algorithm were shown to produce a final adjusted column which globally maximises the cost functional

$$F[\alpha] = -\int_{p_0}^{p_{\rm top}} e^{-\alpha p}\theta(p)\,{\rm d}p, \tag{8}$$

in a more numerically efficient way than the Munkres algorithm (henceforth we use the term 'global maximum' to refer to these solutions). This functional is constructed such that as α gets larger the optimal solution will maximise over rearrangements of $\theta(p)$ with priority given to the top of the column. The algorithm developed in Cheng et al. (2017a) is similar to the top-down algorithm (Wong et al. 2016; Saenz et al. 2015; Harris and Tailleux 2018) and the greedy algorithm (Stansifer et al. 2017; Harris and Tailleux 2018), both of which were developed to determine the global maximum/minimum of some similar cost functional. As this adjustment algorithm finds the global maximum rearrangement of parcels we term it the *global moist convective adjustment algorithm* (GMCAA).

While the GMCAA of Cheng et al. (2017a) is fast and effective ($O(N^2)$ efficient where N is the number of parcels in the column), it may be that adjusting the column towards a global maximum of (8) might not be the most meteorologically appropriate solution. It was speculated in Cheng et al. (2017a) that the GMCAA could be most appropriate when simulating deep convection events, due to the large amount of moisture removed from the system, but it might not be as suitable for shallow convection events in the atmosphere (convective instability), where an alternative arrangement of parcels that releases less moisture, and hence introduces less thermal energy to the parcels, might be more appropriate. In this article we consider two further algorithms based upon swapping neighbouring parcels to identify whether other significant stable rearrangements of the same initial data are possible. As these algorithms are based on swapping neighbouring parcels we term them *parcel swapping moist convective adjustment algorithms* (PSMCAA). While the GMCAA sorts all parcels simultaneously with no defined order of moving the parcels, the PSMCAA essentially assigns an order in which the parcels move so as to reach a stable configuration that simultaneously satisfies $q \le Q_{\rm sat}$ throughout the column. Potentially there are many different ways to determine the order of the parcel swaps leading to subtly different results. To highlight the different rearrangement possibilities we consider two parcel swap algorithms. PSMCAA1: a local approach based upon the amount of virtual potential temperature a parcel can gain by swapping with its neighbour. We swap parcels in the order based on the magnitude of this gain, moving the parcel gaining the most virtual potential temperature first. PSMCAA2: a global approach based upon the largest gain in the functional (8), with θ replaced by θ_v. We again move first the parcel which increases (8) the most.

PSMCAA1 and PSMAA2 give a parameterization of the latent heating processes given in §2 where the adjustment acts to ensure that the column atmosphere is statically stable (3), with no parcels supersaturated ($q \le Q_{\rm sat}$). The column is divided into N equally sized pressure parcels

$$\widetilde{p}_i = p_0 + (p_{\rm top} - p_0)\frac{(i-1/2)}{N}, \tag{9}$$

for $i = 1,...,N$. Each parcel contains an equal mass $\Delta p/g$ of air, where $\Delta p = (p_0 - p_{\rm top})/N$, and the subscripts i denote the Eulerian position of the parcel in the column, not its Lagrangian label. In order to clarify the situation, we use a tilde over variables to denote that it is an Eulerian location. Therefore the pre-adjusted state of the parcels at levels $\widetilde{p}_1$, $\widetilde{p}_2$,..., $\widetilde{p}_N$ have virtual potential temperatures $\widetilde{\theta}^0_1$, $\widetilde{\theta}^0_2$,..., $\widetilde{\theta}^0_N$, specific humidities $\widetilde{q}^0_1$, $\widetilde{q}^0_2$,..., $\widetilde{q}^0_N$ and Lagrangian position labels A^0_1, A^0_2, ..., A^0_N. Note we have neglected the subscript v on $\widehat{\theta}_v$ for simplicity. The Lagrangian labels are solely used as a marker to track the new locations of the parcels in the column after the adjustment process, and this helps in identifying how far parcels have ascended the column. PSMCAA1 is given below.

—START—

In PSMCAA1 the superscript '0' denotes the initial pre-adjusted state, the superscript '1' denotes the final adjusted state, the superscript 'Temp' denotes a temporary value during the switching phase, and the superscript '*I*' on $\widetilde{\theta}$ denotes the potential temperature increase of swapping neighbouring parcels. PSMCAA1 then proceeds as follows:

1. Convert the virtual potential temperatures to absolute temperatures $\widetilde{T}^0_j = \widetilde{\theta}\left(\frac{p}{p_0}\right)^{R/c_p}/(1+0.608\widetilde{q}^0_j)$, and set the temporary variables equal to the pre-adjusted state, $\widetilde{T}^{\rm Temp}_j = \widetilde{T}^0_j$, $\widetilde{q}^{\rm Temp}_j = \widetilde{q}^0_j$, $A^{\rm Temp}_j = A^0_j$ for $j = 1,...,N$. If any parcels are initially supersaturated, then condense any excess moisture, and heat the parcel by solving

$$\widehat{T}_j\left(\frac{p_0}{\widetilde{p}_j}\right)^{R/c_p}\exp\left(\frac{LQ_{\rm sat}(\widehat{T}_j,\widetilde{p}_j)}{\widehat{T}_j}\right) - \frac{\widetilde{\theta}^0_j}{(1+0.608\widetilde{q}^0_j)}\exp\left(\frac{L\widetilde{q}^0_j}{\widetilde{T}^0_j}\right) = 0,$$

for $\widehat{T}_j$ and set $\widetilde{T}^{\rm Temp}_j = \widehat{T}_j$ and $\widetilde{q}^{\rm Temp}_j = Q_{\rm sat}(\widehat{T}_j,\widetilde{p}_j)$. Convert absolute temperatures back to virtual potential temperatures $\widetilde{\theta}^{\rm Temp}_j$ using (1).

2. Calculate the virtual potential temperature increase of each parcel at $\widetilde{p}_j$ if it swaps with its above neighbour at $\widetilde{p}_{j+1}$, for $j = 1,...,N-1$.

   (a) **If** $\widetilde{q}_j^{\text{Temp}} = Q_{\text{sat}}(\widetilde{T}_j^{\text{Temp}}, \widetilde{p}_j)$ (i.e. parcel is saturated) then excess moisture will condense during the swap, latent heat will be released, and its virtual potential temperature will change. Its new absolute temperature $\widehat{T}_j$ is found by solving the implicit relation

$$\widehat{T}_j \left(\frac{p_0}{\widetilde{p}_{j+1}}\right)^{R/c_p} \exp\left(\frac{LQ_{\text{sat}}(\widehat{T}_j, \widetilde{p}_{j+1})}{\widehat{T}_j}\right) - \frac{\widetilde{\theta}_j^{\text{Temp}}}{(1+0.608\widetilde{q}_j^{\text{Temp}})} \exp\left(\frac{L\widetilde{q}_j^{\text{Temp}}}{\widetilde{T}_j^{\text{Temp}}}\right) = 0,$$

   and its moisture level is then

$$\widehat{q}_j = Q_{\text{sat}}(\widehat{T}_j, \widetilde{p}_{j+1}), \tag{10}$$

   with Lagrangian label $\widehat{A}_j = A_j^0$. The virtual potential temperature increase is defined as $\widetilde{\theta}_j^I = \widehat{\theta}_j - \widetilde{\theta}_{j+1}^{\text{Temp}}$, for $j = 1,...,N-1$, where $\widehat{\theta}_j = \widehat{T}_j(1+0.608\widehat{q}_j)\left(\frac{p_0}{\widetilde{p}_{j+1}}\right)^{R/c_p}$.

   (b) **If** $\widetilde{q}_j^{\text{Temp}} < Q_{\text{sat}}(\widetilde{T}_j^{\text{Temp}}, \widetilde{p}_j)$ (i.e. the parcel is unsaturated) then there is no latent heat exchange and the parcel at $\widetilde{p}_j$ rises adiabatically. If during this swap the parcel becomes supersaturated, then rain out excess moisture as in step 1. Then $\widehat{\theta}_j = \widetilde{\theta}_j^{\text{Temp}}$, $\widehat{q}_j = q_j^{\text{Temp}}$, $\widehat{A}_j = A_j^{\text{Temp}}$ and the virtual potential temperature increase is $\widetilde{\theta}_j^I = \widetilde{\theta}_j^{\text{Temp}} - \widetilde{\theta}_{j+1}^{\text{Temp}}$.

3. The process in 2 above, generates an array of virtual potential temperature increases $\widetilde{\theta}_j^I$ for $j = 1,...,N-1$. We then determine $\max(\widetilde{\theta}_j^I)$, which occurs at $j = J$, say.

   (a) **If** $\widetilde{\theta}_J^I > 0$ then the parcel at $\widetilde{p}_J$ can gain enough virtual potential temperature to switch places with the parcel at $\widetilde{p}_{J+1}$, hence we switch these two parcels and re-label

$$\widetilde{\theta}_J^{\text{Temp}} = \widetilde{\theta}_{J+1}^{\text{Temp}}, \quad \widetilde{q}_J^{\text{Temp}} = \widetilde{q}_{J+1}^{\text{Temp}}, \quad A_J^{\text{Temp}} = A_{J+1}^{\text{Temp}},$$
$$\widetilde{\theta}_{J+1}^{\text{Temp}} = \widehat{\theta}_J, \qquad \widetilde{q}_{J+1}^{\text{Temp}} = \widehat{q}_J, \qquad A_{J+1}^{\text{Temp}} = \widehat{A}_J$$

   (b) **If** $\widetilde{\theta}_J^I \le 0$ then no parcels can gain enough virtual potential temperature to switch places with their neighbours, hence the algorithm stops and we define

$$\widetilde{\theta}_j^1 = \widetilde{\theta}_j^{\text{Temp}}, \quad \widetilde{q}_j^1 = \widetilde{q}_j^{\text{Temp}}, \quad A_j^1 = A_j^{\text{Temp}} \quad \text{for} \quad j = 1,...,N.$$

4. Steps 2 and 3(a) are repeated until case (3)(b) arises.

—END—

For PSMCAA2 the algorithm is essentially that of PSMCAA1 except in parts 2(a) and (b) we also calculate $F_j^I = F_S - F_{PS}$ where F is the numerical value of (8) (with $\theta \mapsto \theta_v$, and $\alpha = 0.007$ as in Cheng et al. (2017a)). Here F_S is the value of the functional after the parcel swap and F_{PS} is the value of the functional prior to the swap. Thus in part 3 it is $F_J^I = \max(F_j^I)$ which determines the order of the swaps, rather than $\widetilde{\theta}_J^I$. PSMCAA2 continues until $F_J^I \le 0$, and if $F_J^I > 0$ this also means that $\widetilde{\theta}_J^I > 0$, hence the CIC is correctly implemented. Essentially PSMCAA2 places a larger weighting on parcel swaps which are higher up the column. This can be most simply seen by considering two parcel swaps which lead to the same value of $\widetilde{\theta}_J^I$. In PSMCAA1 these are given equal weight and so we can choose which pair to swap first (our algorithm swaps the lower pair first), but in PSMCAA2 the exponential weighting factor in (8) prioritises the higher pair. The two algorithms become identical if the exponential weighting function is replaced by a linear function of p.

For a time-dependent convection problem consisting of a rising air column as considered in Cheng et al. (2017b), it was shown that including the CIC in the calculation was essential for proving well-posedness of the problem. Because the GMCAA sorts all parcels simultaneously, identifying the exact level at which two parcels overtake (or pass) each other is difficult, as such the GMCAA assumes that if a saturated parcel needs to 'overtake' another saturated parcel as they both rise, then they meet at a height where this overtake can happen (Cheng et al. 2017a). However, the parcels may be moved around by other parcels rising above them, so the way we implement the CIC in a physically sound way is to define an order in which the parcels swap, as in PSMCAA1 and PSMCAA2.

In §4 we present results which compare adjustments of an idealized atmosphere via the GMCAA and PSMCAA1 and PSMCAA2. In order to present these results (most clearly in a semi-analytical manner, in contrast to a fully numerical approach), an explicit form for Q_{sat} is required, which we take from the empirical formula given in Gill (1982),

$$Q_{\text{sat}}(T,p) = \frac{Q_0}{p} e_{\text{sat}}(T). \tag{11}$$

Here Q_0 is a positive constant and $e_{\text{sat}}(T)$ is the saturation vapour pressure of water,

$$\log_{10}(e_{\text{sat}}) = \frac{Q_1 + Q_2[T - T_0]}{1 + Q_3[T - T_0]},$$

where Q_1, Q_2, Q_3 and T_0 are positive constants (Gill 1982, p606), whose values can be found in table 1. Values of e_{sat} using the form above agree with those in the

parameter	value	units
Q_0	62.20000	Pa
Q_1	0.78590	K
Q_2	0.03477	—
Q_3	0.00412	—
Q_4	0.00422	—
T_0	273	K

TABLE 1. Parameter values in (12) used for the numerical simulations of §4.

Smithsonian Meteorological Tables to within 0.2% for $233 \leq T \leq 313$K. For the examples presented in this article, we have $T < 233$K at the very top of the atmosphere, hence there is a slightly larger error in the values of $e_{\rm sat}$ in this region. Combining the above two formulae leads to

$$Q_{\rm sat}(T,p) = \frac{Q_0}{p} 10^{\left\{ \frac{Q_1+Q_2[T-T_0]}{1+Q_3[T-T_0]} \right\}}. \qquad (12)$$

4. Non-uniqueness Results

In this section we present two idealized examples for the adjustment of an unstable column of moist air and compare the results of the algorithms discussed in §3. We also examine the robustness of the algorithms to the form of the initial pre-adjusted state. For all the results in this section we use $N = 1000$ parcels, and $p_0 = 10^5$ Pa at the Earth's surface.

a. Example A

In Example A we consider a column whose instability has been triggered by the inequality (3) being violated close to the planetary surface (i.e. the column is buoyantly unstable). We consider this example as one where the surface of the Earth, in the tropics for example, has been heated leaving a warm but moist layer at the bottom of the column. The initial potential temperature and relative humidity distributions we use are

$$\theta^0(p) = f(p) \exp\left(\frac{3}{5} \left[1 - \left(\frac{p}{p_0} \right)^{R/c_p} \right] \right), \qquad (13)$$

where

$$f(p) = \begin{cases} 300 - \Theta \sin\left(\frac{35}{3} \pi \left[1 - \left(\frac{p}{p_0} \right)^{R/c_p} \right] \right) \\ \qquad \text{for } p > p_0 \left(\frac{67}{70} \right)^{cp/R} \text{kPa} \\ 300 - \Theta \\ \qquad \text{for } p < p_0 \left(\frac{67}{70} \right)^{cp/R} \text{kPa} \end{cases}, \qquad (14)$$

and

$$q^0(p) = \begin{cases} Q_{\rm sat}(T^0,p) & \text{if } p > 85\,\text{kPa} \\ Q_{\rm sat}(T^0,p) \exp\left(\frac{p-85000}{5000} \right) & \text{if } p < 85\,\text{kPa} \end{cases}, \qquad (15)$$

respectively. Here T^0 is the initial absolute temperature distribution found from (13). A plot of the initial pre-adjusted form of the virtual potential temperature $\theta_v^0 = (1 + 0.608 q^0)\theta^0$, when $\Theta = 8$ K, and q^0 is given in figure 1. In (14) we leave Θ as a parameter so that we can use this same potential temperature distribution for Example B in §4b but with a different value of Θ.

In figure 2 we consider the forms of $\theta_v(z)$ and $q(z)$ post-adjustment for (a,b) PSMCAA1, (c,d) PSMCAA2 and (e,f) the GMCAA. We observe that PSMCAA1 adjusts to essentially the same solution as the GMCAA. The structure of the solution is a weak solution consisting of saturated and dry parcels interleaving throughout the column. This type of weak solution, and its consequences for standard numerical techniques, was discussed in Cheng et al. (2017a). The adjustment of the column using PSMCAA2 has a slightly different structure. While there is still an interleaving of moist and dry parcel layers, this time the parcels are unsaturated, except at the very top of the column. There is also fractionally more latent heating at the bottom of the column. The reason for the difference between the two parcel swapping algorithms is in the order that the parcels are swapped. In PSMCAA1 the parcels move from approximately the bottom of the column first, and these parcels contain more moisture, hence produce most latent heat when ascending. Therefore these parcels ascend highest in the column. This can be seen in the initial and final Lagrangian levels of the parcels in figure 3. Then as parcels originally above the parcels which have already ascended begin to rise, they do not ascend as far in the column and thus remain saturated. However, as noted earlier the exponential weighting factor in the cost function puts more emphasis on the parcels at the top of the column, thus these parcels move first in PSMCAA2. Therefore, when a lower parcel ascends (and note it will ascend to a higher level) it overtakes the first parcel to move, forcing that first parcel back down the column, so that it becomes unsaturated, because its virtual potential temperature does not change but its height does. Note, it could become saturated again if re-absorption of precipitation was included in the model.

Even in this simple example we observe that PSMCAA1 and PSMCAA2 produce different adjustments of the column, corresponding to different maxima of (8). Hence there is a non-uniqueness to the adjustment problem depending on the ordering of parcel swaps. This demonstrates that parcel rearrangement order matters. However, as PSMCAA1 and the GMCAA produce qualitatively very similar results, it can be argued that PSMCAA1 is the parcel swapping algorithm which most accu-

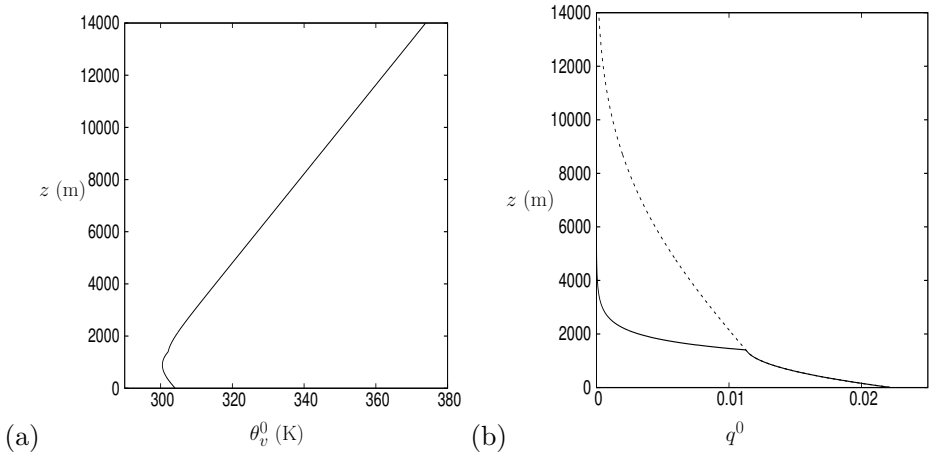

FIG. 1. Plot of (a) the initial virtual potential temperature distribution $\theta_v^0(z) = \theta^0(1+0.608q^0)$ with θ^0 given by (13) with $\Theta = 8$ K and (b) the initial humidity distribution $q^0(z)$ given by (15). In panel (b) the dashed line gives the value of Q_{sat}.

rately models the physics occurring in the atmosphere. In Example B we demonstrate that, in contrast to the above, PSMCAA1 and GMCAA adjustments can lead to significantly different column adjustments for alternative initial data sets.

b. Example B

In Example B we consider a column in which the instability is triggered by the lower layer of air near the Earth's surface becoming supersaturated but with an almost stable virtual potential temperature distribution ((3) is broken for only the bottom 200 m of the column). This example can be considered as the case of a column of air being lifted as it passes over hilly topography, or as a front of cold air penetrates underneath (Cheng et al. 2017a). The initial potential temperature distribution is again given by (13) except we choose $\Theta = 4$ K such that the profile almost satisfies (3) and the initial relative humidity distribution is

$$q^0(p) = \begin{cases} 1.05 Q_{\text{sat}}(T^0, p) & \text{if } p > 85\,\text{kPa} \\ 1.05 Q_{\text{sat}}(T^0, p) \exp\left(\frac{p-85000}{5000}\right) & \text{if } p < 85\,\text{kPa} \end{cases} \tag{16}$$

In this case the moist layer is a modest 5% supersaturated, and hence the column is marginally unstable, but this is sufficient to highlight non-uniqueness in the system. Plots of the initial θ_v^0 and q^0 profiles are given in figure 4.

In figure 5 we again compare the final adjustments of the three algorithms. The GMCAA in panels (e,f) rains out a large volume of moisture, producing a weak solution with interleaving saturated and unsaturated parcels through the column. Because of the large amount of condensation, a large amount of latent heating of the column has occurred. The adjustment via PSMCAA1 in panels (a,b) is significantly different. While this adjustment has a similar moist layer to the GMCAA for $6000\,\text{m} \leq z \leq 8000\,\text{m}$, the lower layer contains more moisture (less condensation has occurred), and hence this lower layer is cooler than the result in panel (e). By considering the initial and final levels of the individual parcels in figure 6 we see that fewer parcels rise up the column for PSMCAA1 in this example compared to the GMCAA algorithm. The parcels in the lower moist layer are unsaturated, suggesting that these parcels ascended the column first, and then were overtaken by the parcels which ascended to the top moist layer. In this case, because the initial θ_v^0 profile is almost stable, once the parcels at the bottom of the column are chosen to ascend, this choice forces all the saturated parcels above those chosen down the column, making them unsaturated and unable to rise. In the GMCAA, because all parcels are sorted simultaneously, and without a defined order, when a parcel at the bottom of the column is installed into its adjusted position, all the other saturated parcels are assumed to remain saturated and at their pre-adjusted positions until they are sorted. The results of the PSMCAA2 in panels (c,d) have a similar structure to the PSMCAA1 results except that the upper layer parcels are not saturated throughout this upper layer, and both are at slightly higher levels in the column.

The results in Examples A and B show that the moist convective adjustment problem does not have a unique (stable) solution for every choice of initial data, and that the order in which parcels are swapped during the adjustment is significant to the final adjusted outcome. The scenarios in Example A showed that for some initial data PSMCAA1 and GMCAA adjust to the same result, the global maximum of (8), while in Example B PSMCAA1 found a local maximum of (8) solution with less total latent heating of column parcels. In both examples PSMCAA2 demonstrates that the parcel rearrangement order matters, although given the agreement between PSM-

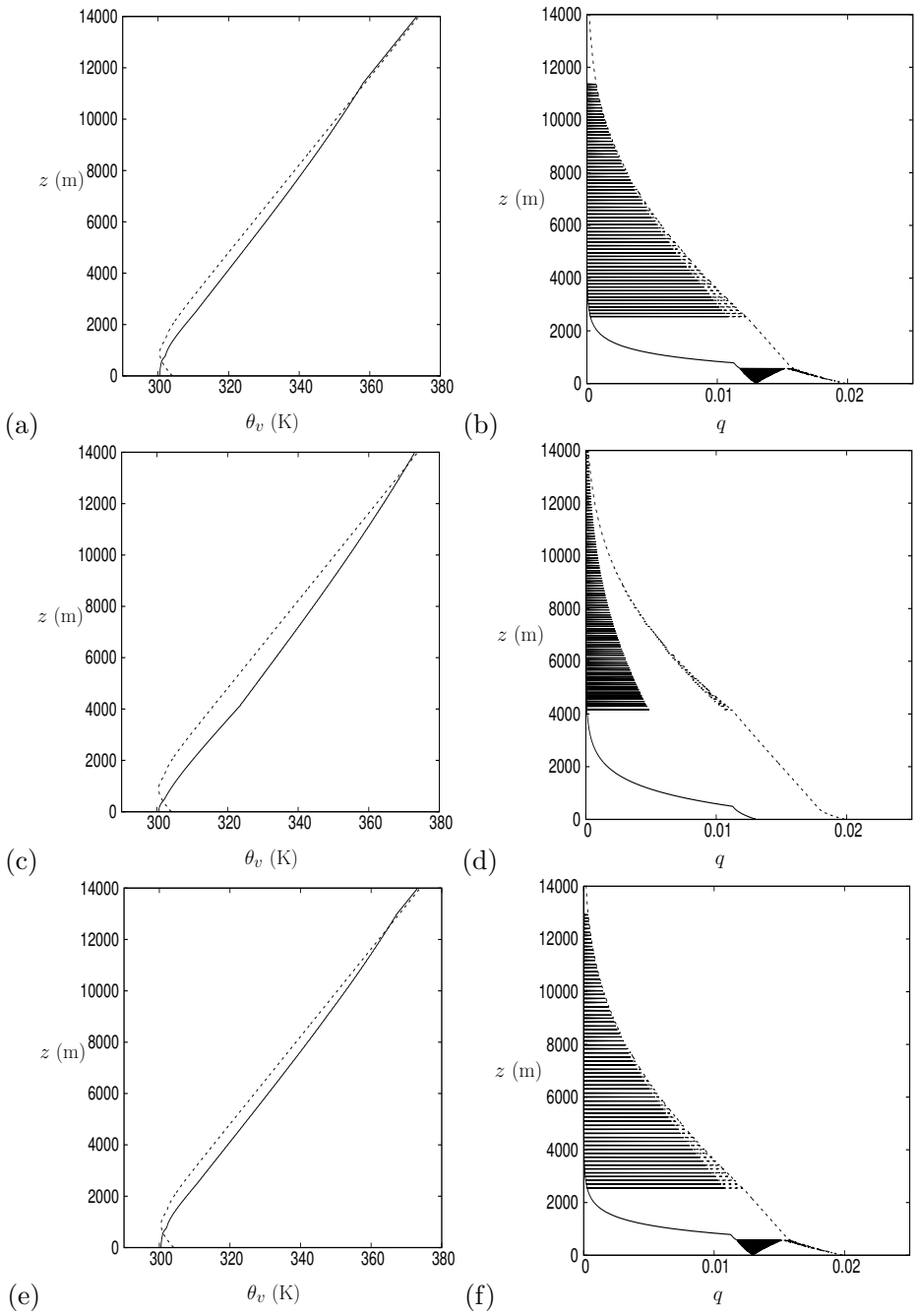

FIG. 2. Plot of (a,c,e) the virtual potential temperature post-adjustment $\theta_v(z)$ (solid line) and pre-adjustment $\theta_v^0(z)$ (dashed line) and (b,d,f) the moisture distribution $q(z)$ post-adjustment for the pre-adjusted state given in figure 1. Panels (a,b) are adjusted via PSMCAA1, (c,d) via PSMCAA2 and (e,f) via GMCAA.

CAA1 and GMCAA in Example A, it is likely that the algorithm for PSMCAA1 gives a better representation of the physics in an actual model atmosphere. Therefore, if two (or more) locally stable adjustment solutions exist for the same pre-adjusted state (that is, initial data) then the sensible question to ask is 'which solution should my NWP model be adjusting to?'

The column adjustment problems in these two examples can be considered as one time-step in an inner loop of a time-dependent problem such as that of a rising col-

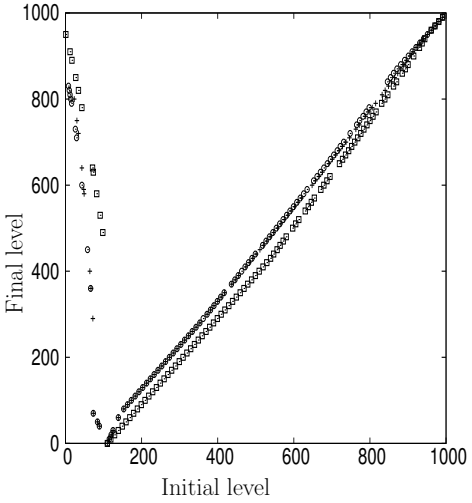

FIG. 3. Plot of the final Eulerian position of each parcel compared to its initial level in the corresponding results of figure 2. In each panel the circles represent results of PSMCAA1, squares represent PSMCAA2 and the crosses represent the GMCAA. We plot only every 10 points so as not to congest the figures.

umn of atmosphere moving over a mountain range (see Cheng et al. (2017a)), or of a NWP simulation. In either case, assuming that significantly different local and global adjustments exist, if the model continuously adjusts to the global solution then the NWP simulation will predict a large amount of moisture release, in a short amount of time, and hence a large amount of local latent heating of air parcels. This in turn will feed in to the background horizontal dynamics of the NWP model and could lead to an over prediction of precipitation, wind velocities and temperatures etc. On the other hand, if the model always adjusts to the local solution at each time-step then the amount of moisture released will be less, and potentially released more slowly, so there will be less thermal energy to feed back into the background dynamics. These alternatives may ultimately lead to very different global solutions. Hence care is needed when running such NWP and climate models to make sure the model is directed to the more appropriate solution.

c. Model sensitivity analysis

In this section we re-consider the column adjustment from Example A, but here in figure 7 we compare the three results with $\Theta = 8\,\mathrm{K}$, $\Theta = 6\,\mathrm{K}$ and $\Theta = 4\,\mathrm{K}$ in order to demonstrate the robustness of the results, i.e. that the results are not sensitive to the initial pre-adjusted state. Note that as Θ is reduced the overall stability of the column, as identified by (3), increases in the sense that for $\Theta = 4\,\mathrm{K}$ the column is only unstable for approximately the lowest 200 m, as noted in §4b. In the results which follow we only plot the post-adjusted moisture distribution as this is the clearest indicator of the structure of the resulting adjustment solution, and we only consider PSMCAA1 as, from the preceding results in §a and §b, this algorithm appears to give the best representation of the physics in a more realistic atmosphere.

The results in figure 7 show that the adjusted states for PSMCAA1 and GMCAA with $\Theta = 8\,\mathrm{K}$ and $\Theta = 6\,\mathrm{K}$ agree very well with each other, i.e. the parcel swap algorithm adjusts to the same state as the global algorithm. Also, the $\Theta = 6\,\mathrm{K}$ solution has a qualitatively similar structure to that of the $\Theta = 8\,\mathrm{K}$ solution, showing that the adjustment algorithms are robust and not sensitive to the initial pre-adjusted state. The results for $\Theta = 4\,\mathrm{K}$ in panels (e) and (f) again show the non-uniqueness of the solution: compared to figure 5, the PSMCAA1 result here has no lower moist layer. These results show that there is a smooth transition from the results in panels (c,d) to those in panels (e,f), but that the PSMCAA1 changes from the global to a local solution when the local forms, while the GMCAA continues to adjust to the global maximum of (8).

In figure 8 we consider one final test on the robustness of the solutions by considering the cases in figure 7 but with an additional layer of moist saturated parcels ($q = Q_{\mathrm{sat}}$) placed in the pre-adjusted state for $48 \leq p \leq 55\,\mathrm{kPa}$. This additional region of moist parcels is an example of an existing cloud layer in the mid-Troposphere, which has the potential to stop some rising parcels from passing through it, as well as acting as an additional region of convection. The results presented here are consistent with those in figure 7, with the $\Theta = 8\,\mathrm{K}$ and $6\,\mathrm{K}$ results adjusting to the global solution while the $\Theta = 4\,\mathrm{K}$ result demonstrates the non-uniqueness in the problem. Again the similarities of the $\Theta = 8\,\mathrm{K}$ and $6\,\mathrm{K}$ results show that the adjustment results are not in general sensitive to the initial pre-adjusted state.

5. Conclusion and discussion

This article investigates moist convection of warm, moist air in a single-column atmosphere (which has no horizontal variation of any variable). The convection is modelled using conservation laws for the virtual potential temperature θ_v and equivalent potential temperature θ_e (which measure the thermal energy of unsaturated and saturated air parcels respectively - see Emanuel (1994)), the air mass, and the moisture mass. We construct two numerical moist convective adjustment algorithms based upon swapping neighbouring air parcels: each algorithm allows saturated air parcels to rise up the column to their neutral buoyancy level (following their moist adiabat). Each algorithm swaps parcels: the first via a local approach with the parcel choice being that with the largest gain in virtual potential temperature during swapping; and the second a

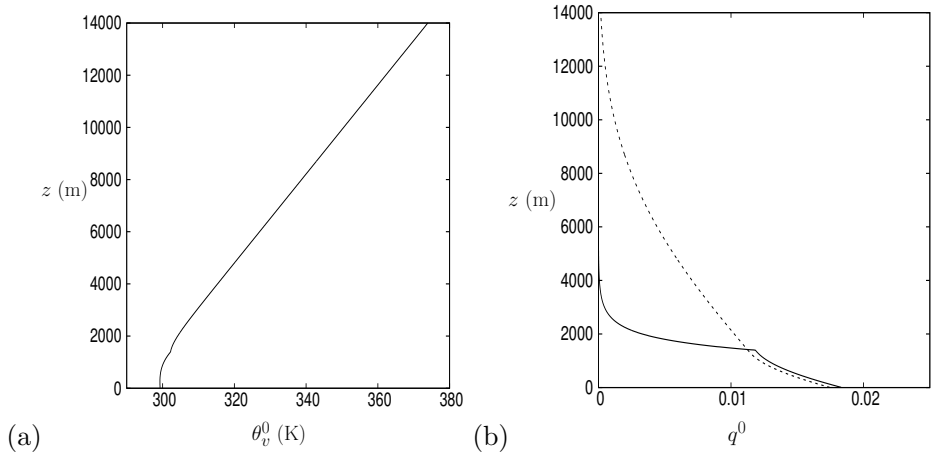

FIG. 4. Plot of (a) the initial virtual potential temperature distribution $\theta_v^0(z) = \theta^0(1+0.608q^0)$ with θ^0 given by (13) with $\Theta = 4$ K and (b) the initial humidity distribution $q^0(z)$ given by (15). In panel (b) the dashed line gives the value of Q_{sat}.

global approach with the parcel swap making the largest gain in the cost functional (8) being actioned first. These algorithms are based on the physical conservation laws that underpin the usual differential equations that model weather evolution. The algorithms also include the convective inhibition criterion (CIC) (Colby Jr 1984), where parcels only swap places if the lower parcel has sufficient buoyancy (arising from condensing water vapour and consequent latent heating of the air parcel) to vertically move it above the higher parcel.

The results of these parcel swapping adjustment algorithms are compared directly with the results of the adjustment algorithm devised in Cheng et al. (2017a) in two examples A, B by choosing initial data that corresponds to weather scenarios known as deep or shallow convection. The Cheng et al. (2017a) adjustment algorithm produces a large amount of latent heating of parcels which arises from the condensation of a large amount of water vapour: the algorithm produces a rearrangement of the air parcels which globally maximizes (8). In Example A, the column is initially buoyantly unstable and our local parcel swapping algorithm produces a near identical adjustment of the column to the global maximizing algorithm of Cheng et al. (2017a). However, in the marginally, or weakly, unstable case of the initial data of Example B, the two algorithms give significantly different results. The global algorithm produces a result more similar to that in Example A, where many parcels rise relatively large distances within the column giving a moisture profile with interleaving saturated and unsaturated parcel layers. By contrast the local parcel swapping algorithm has fewer parcels rising from the bottom of the column, giving a much smaller total amount of condensation and hence a smaller total amount of latent heating of parcels within the column. The results in Example B show that there are potentially multiple adjustments of a practical atmospheric column, where the initial data is chosen from realistic atmospheric forecasting situations. Therefore, if forecasting numerical codes (NWP) are always designed to adjust to the global maximum of (8) solution then it might turn out that this is not the desired solution, and which solution is more appropriate depends upon additional information, such as fine detail of the velocity, temperature and moisture distributions in the horizontal directions around the column. The consequence of this result for numerical weather prediction codes and climate models is that unstable vertical convection has to be numerically guided to the (meteorological or climate) desired solution depending upon both local and global features of the flow. As a bonus, we discover new types of finely layered, in the vertical, solutions, where drier layers are interleaved with moist layers, as shown in figures 2(b), (d) and (f), between the approximate heights of $3000 - 12\,000$m.

The single-column model presented here gives insight into how a heated, moist column of compressible atmosphere adjusts when perturbed from a stable vertical arrangement to an unstable one. This model can be directly extended to time-dependent problems, such as the lifted column problem in Cheng et al. (2017a), where radiative cooling and sources of moisture and/or heat are significant. The main point of this work is to show how a modified parcel adjustment algorithm finds different stable solutions to those usually published in the literature. These different solutions mathematically are local maximisers, not the usual global maximisers, of an associated cost/energy functional. These new solutions generate less precipitation and hence can be thought of as shallow convection in the weather forecasting literature. Since shallow convection is widely present in both global weather forecasting and in climate prediction models, the message

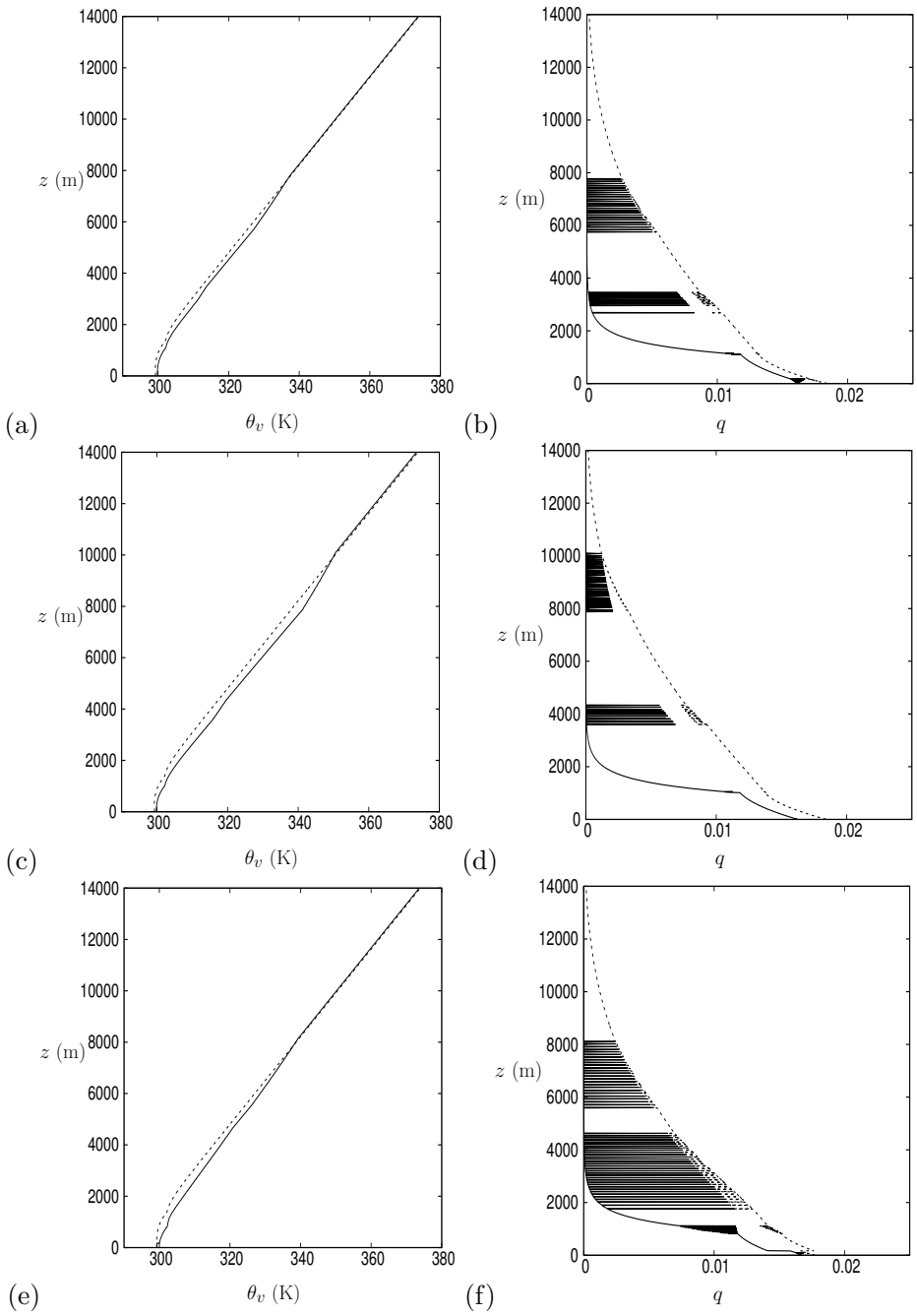

FIG. 5. Plot of (a,c,e) the virtual potential temperature post-adjustment $\theta_v(z)$ (solid line) and pre-adjustment $\theta_v^0(z)$ (dashed line) and (b,d,f) the moisture distribution $q(z)$ post-adjustment for the pre-adjusted state (13) and (16) with $\Theta = 4$ K. Panels (a,b) are adjusted via PSMCAA1, (c,d) via PSMCAA2 and (e,f) via GMCAA.

from the above examples is that careful thought is required when guiding numerical forecasting code in the presence of moist convection.

Acknowledgement

The authors thank the editor and the referees for their helpful comments which significantly improved this manuscript.

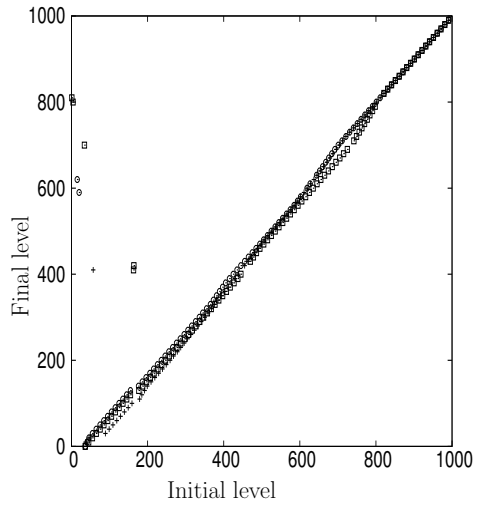

FIG. 6. Plot of the final Eulerian position of each parcel compared to its initial level in the corresponding results of figure 5. In each panel the circles represent results of PSMCAA1, squares represent PSMCAA2 and the crosses represent the GMCAA. We plot only every 10 points so as not to congest the figures.

References

Arakawa, A., 2004: The cumulus parameterization problem: Past, present, and future. *J. Climate*, **17 (13)**, 2493–2525.

Betts, A. K., and C. Jakob, 2002: Study of diurnal cycle of convective precipitation over Amazonia using a single column model. *J. Geophys. Res.*, **107**, 4732.

Bokhove, O., and M. Oliver, 2006: Parcel Eulerian–Lagrangian fluid dynamics of rotating geophysical flows. *Proc. R. Soc. London A*, **462 (2073)**, 2575–2592.

Bretherton, C. S., 2007: Challenges in numerical modeling of tropical circulations. *The Global Circulation of the Atmosphere (edited by Schneider, T. and Sobel, A. H.)* (Princeton University Press), 302–330.

Cheng, B., M. J. P. Cullen, J. G. Esler, J. Norbury, M. R. Turner, J. Vanneste, and J. Cheng, 2017a: A model for moist convection in an ascending atmospheric column. *Q. J. R. Meteorol. Soc.*, **143 (708)**, 2925–2939.

Cheng, J., B. Cheng, M. J. P. Cullen, J. Norbury, and M. R. Turner, 2017b: A Rigorous Treatment of Moist Convection in a Single Column. *SIAM J. Num. Anal.*, **49 (5)**, 3854–3892.

Colby Jr, F. P., 1984: Convective inhibition as a predictor of convection during ave-sesame ii. *Mon. Wea. Rev.*, **112 (11)**, 2239–2252.

D'Andrea, F., P. Gentine, A. K. Betts, and B. R. Lintner, 2014: Triggering deep convection with a probabilistic plume model. *J. Atmos. Sci.*, **71 (11)**, 3881–3901.

Emanuel, K. A., 1994: *Atmospheric convection*. Oxford University Press on Demand.

Ghan, S., and Coauthors, 2000: A comparison of single column model simulations of summertime midlatitude continental convection. *J. Geophys. Res.*, **105 (D2)**, 2091–2124.

Gill, A. E., 1982: *Atmosphere-ocean dynamics*. Academic Press (London and Singapore).

Gregory, D., and P. R. Rowntree, 1990: A mass flux convection scheme with representation of cloud ensemble characteristics and stability-dependent closure. *Mon. Weather Rev.*, **118 (7)**, 1483–1506.

Harris, B. L., and R. Tailleux, 2018: Assessment of algorithms for computing moist available potential energy. *Q. J. R. Meteorol. Soc.*, **144 (714)**, 1501–1510.

Hohenegger, C., and C. S. Bretherton, 2011: Simulating deep convection with a shallow convection scheme. *Atmos. Chem. Phys.*, **11 (20)**, 10 389–10 406.

Holt, M. W., 1989: Semigeostrophic moist frontogenesis in a Lagrangian model. *Dyn. Atmos. Ocean.*, **14**, 463–481.

Houze, R. A. J., 1993: *Cloud dynamics*. Academic Press (Waltham).

Lock, A. M., and J. Norbury, 2011: A column model of moist convection: some exact equilibrium solutions. *Q. J. R. Meteorol. Soc.*, **137 (657)**, 979–991.

Lorenz, E. N., 1979: Numerical evaluation of moist available energy. *Tellus*, **31 (3)**, 230–235.

Madden, R. A., and P. R. Julian, 1971: Detection of a 40–50 day oscillation in the zonal wind in the tropical Pacific. *J. Atmos. Sci.*, **28 (5)**, 702–708.

Mapes, B., and R. Neale, 2011: Parameterizing convective organization to escape the entrainment dilemma. *J. Adv. Model. Earth Syst.*, **3 (2)**, M06 004.

Neiman, P. J., and J. A. Shaw, 2003: Coronas and iridescence in mountain wave clouds over northeastern colorado. *Bull. Amer. Meteor. Soc.*, **84 (10)**, 1373–1386.

Park, S., 2014: A unified convection scheme (UNICON). Part I: Formulation. *J. Atmos. Sci.*, **71 (11)**, 3902–3930.

Pierrehumbert, R. T., 2010: *Principles of planetary climate*. Cambridge University Press.

Randall, D. A., and J. Wang, 1992: The moist available energy of a conditionally unstable atmosphere. *J. Atmos. Sci.*, **49 (3)**, 240–255.

Riemann-Campe, K., K. Fraedrich, and F. Lunkeit, 2009: Global climatology of Convective Available Potential Energy (CAPE) and Convective Inhibition (CIN) in ERA-40 reanalysis. *Atmos. Res.*, **93 (1)**, 534–545.

Saenz, J. A., R. Tailleux, E. D. Butler, G. O. Hughes, and K. I. C. Oliver, 2015: Estimating Lorenz's reference state in an ocean with a nonlinear equation of state for seawater. *J. Phys. Oceanogr.*, **45 (5)**, 1242–1257.

Shutts, G., 1994: The adjustment of a rotating, stratified fluid subject to localized sources of mass. *Q. J. R. Meteorol. Soc.*, **120 (516)**, 361–386.

Shutts, G. J., and M. J. P. Cullen, 1987: Parcel stability and its relation to semigeostrophic theory. *J. Atmos. Sci.*, **44 (9)**, 1318–1330.

Sobel, A. H., and C. S. Bretherton, 2000: Modeling tropical precipitation in a single column. *J. Climate*, **13 (24)**, 4378–4392.

Stansifer, E. M., P. A. O'Gorman, and J. I. Holt, 2017: Accurate computation of moist available potential energy with the Munkres algorithm. *Q. J. R. Meteorol. Soc.*, **143 (702)**, 288–292.

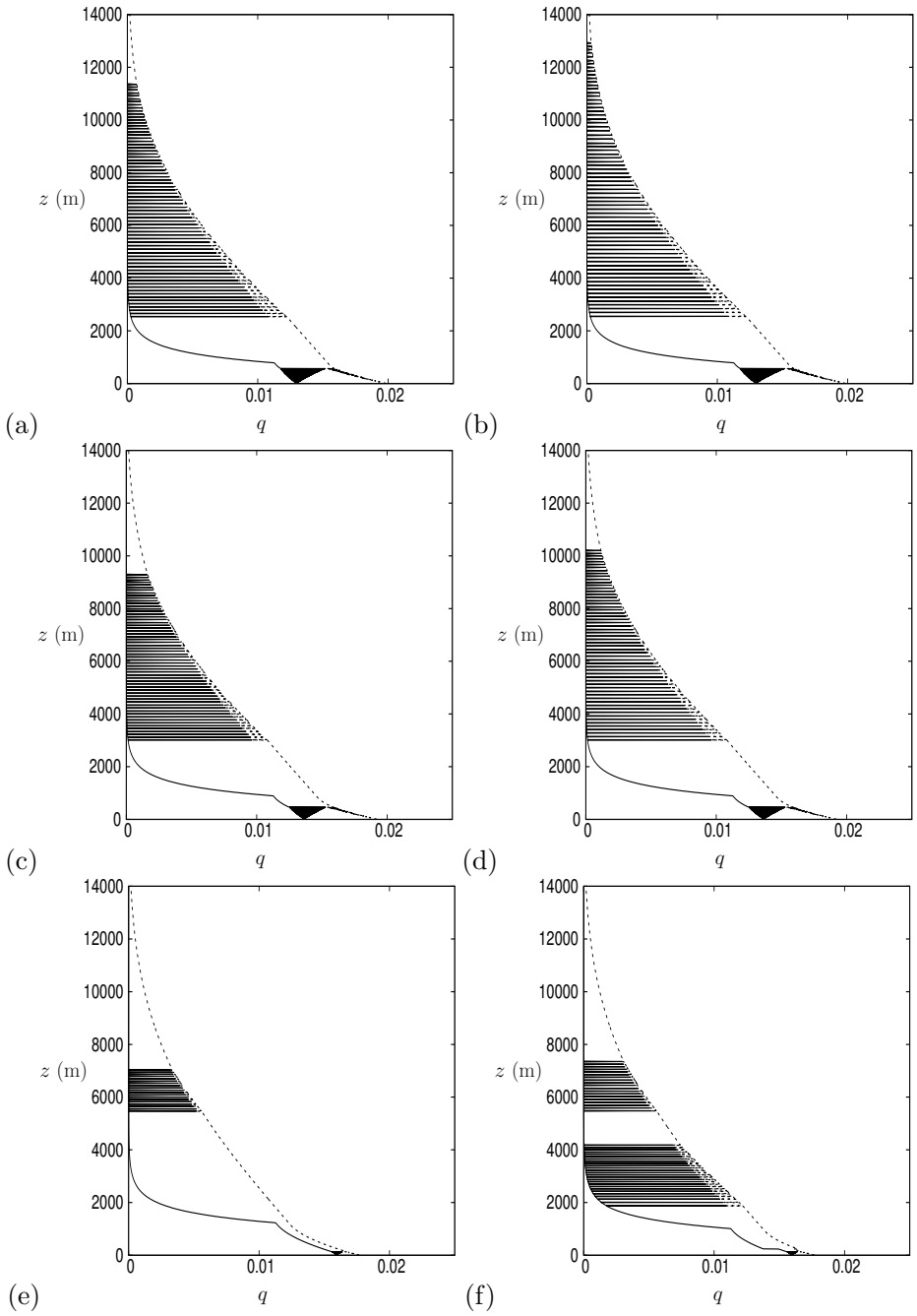

FIG. 7. Plot of the moisture distribution $q(z)$ post-adjustment for the pre-adjusted state (13) and (16) with (a,b) $\Theta = 8\,\mathrm{K}$, (c,d) $\Theta = 6\,\mathrm{K}$ and (e,f) $\Theta = 4\,\mathrm{K}$. Panels (a,c,e) are adjusted via PSMCAA1, and (b,d,f) via GMCAA.

Tiedtke, M., 1989: A comprehensive mass flux scheme for cumulus parameterization in large-scale models. *Mon. Weather Rev.*, **117 (8)**, 1779–1800.

Wang, J., and D. A. Randall, 1994: The moist available energy of a conditionally unstable atmosphere. Part II: Further analysis of GATE data. *J. Atmos Sci.*, **51 (5)**, 703–710.

Whiteman, C. D., 2000: *Mountain meteorology: fundamentals and applications*. Oxford University Press (Oxford).

Wong, K. C., R. Tailleux, and S. L. Gray, 2016: The computation of reference state and APE production by diabatic processes in an idealized tropical cyclone. *Q. J. R. Meteorol. Soc.*, **142 (700)**, 2646–2657.

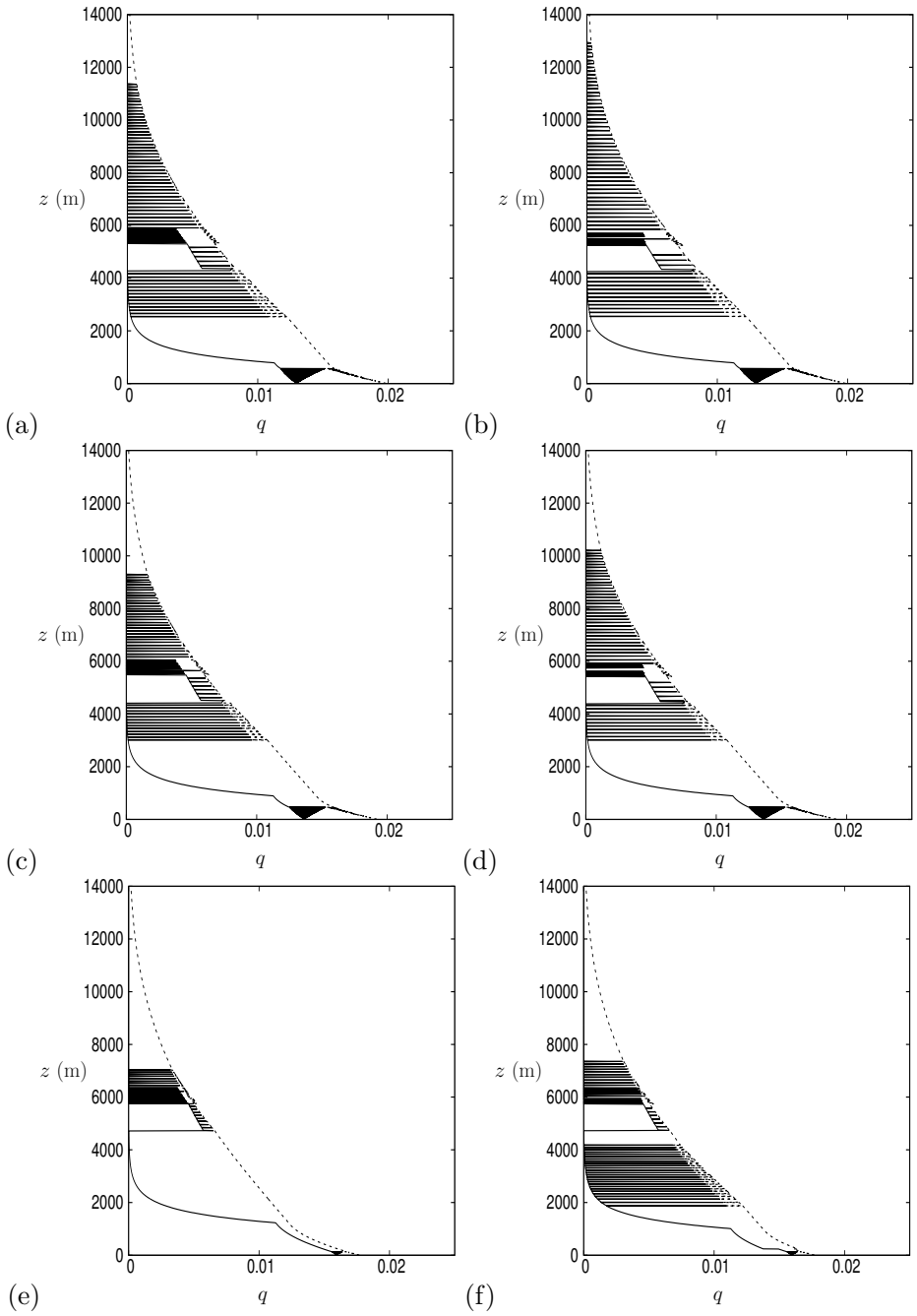

FIG. 8. Plot of the moisture distribution $q(z)$ post-adjustment for the pre-adjusted state (13) and (16) with an additional layer of saturated parcels between 55 kPa and 48 kPa with (a,b) $\Theta = 8$ K, (c,d) $\Theta = 6$ K and (e,f) $\Theta = 4$ K. Panels (a,c,e) are adjusted via PSMCAA1, and (b,d,f) via GMCAA.

Yanai, M., S. Esbensen, and J.-H. Chu, 1973: Determination of bulk properties of tropical cloud clusters from large-scale heat and moisture budgets. *J. Atmos Sci.*, **30 (4)**, 611–627.

Yang, G.-Y., and J. Slingo, 2001: The diurnal cycle in the tropics. *Mon. Wea. Rev.*, **129 (4)**, 784–801.